AFRL-RX-WP-JA-2014-0156

AUTONOMIC COMPOSITE HYDROGELS BY REACTIVE PRINTING: MATERIALS AND OSCILLATORY RESPONSE (POSTPRINT)

R. A. Vaia
AFRL/RXA

NOVEMBER 2013
Interim Report

AIR FORCE RESEARCH LABORATORY
MATERIALS AND MANUFACTURING DIRECTORATE
WRIGHT-PATTERSON AIR FORCE BASE, OH 45433-7750
AIR FORCE MATERIEL COMMAND
UNITED STATES AIR FORCE

NOTICE AND SIGNATURE PAGE

Using Government drawings, specifications, or other data included in this document for any purpose other than Government procurement does not in any way obligate the U.S. Government. The fact that the Government formulated or supplied the drawings, specifications, or other data does not license the holder or any other person or corporation; or convey any rights or permission to manufacture, use, or sell any patented invention that may relate to them.

This report was cleared for public release by the USAF 88th Air Base Wing (88 ABW) Public Affairs Office (PAO) and is available to the general public, including foreign nationals.

Copies may be obtained from the Defense Technical Information Center (DTIC) (http://www.dtic.mil).

AFRL-RX-WP-JA-2014-0156 HAS BEEN REVIEWED AND IS APPROVED FOR PUBLICATION IN ACCORDANCE WITH ASSIGNED DISTRIBUTION STATEMENT.

//Signature//	//Signature//
RICHARD A. VAIA Technical Director Functional Materials Division	TIMOTHY J. BUNNING, Chief Functional Materials Division Materials and Manufacturing Directorate

This report is published in the interest of scientific and technical information exchange, and its publication does not constitute the Government's approval or disapproval of its ideas or findings.

REPORT DOCUMENTATION PAGE

Form Approved
OMB No. 074-0188

1. REPORT DATE (DD-MM-YYYY)	2. REPORT TYPE	3. DATES COVERED *(From – To)*
November 2013	Interim	05 November 2009 – 01 October 2013

4. TITLE AND SUBTITLE
AUTONOMIC COMPOSITE HYDROGELS BY REACTIVE PRINTING: MATERIALS AND OSCILLATORY RESPONSE (POSTPRINT)

5a. CONTRACT NUMBER
In-house

5b. GRANT NUMBER

5c. PROGRAM ELEMENT NUMBER
62102F

6. AUTHOR(S)
(see back)

5d. PROJECT NUMBER
4347

5e. TASK NUMBER

5f. WORK UNIT NUMBER
X03Z

7. PERFORMING ORGANIZATION NAME(S) AND ADDRESS(ES)
(see back)

8. PERFORMING ORGANIZATION REPORT NUMBER

9. SPONSORING / MONITORING AGENCY NAME(S) AND ADDRESS(ES)
Air Force Research Laboratory
Materials and Manufacturing Directorate
Wright Patterson Air Force Base, OH 45433-7750
Air Force Materiel Command
United States Air Force

10. SPONSOR/MONITOR'S ACRONYM(S)
AFRL/RXA

11. SPONSOR/MONITOR'S REPORT NUMBER(S)
AFRL-RX-WP-JA-2014-0156

12. DISTRIBUTION / AVAILABILITY STATEMENT
Approved for public release; distribution unlimited. This report contains color.

13. SUPPLEMENTARY NOTES
PA Case Number: 88ABW-2014-0725; Clearance Date: 25 February 2014. Journal article published in Soft Matter, 2014, 10, 1329. © 2014 The Royal Society of Chemistry. The U.S. Government is joint author of the work and has the right to use, modify, reproduce, release, perform, display or disclose the work. The final publication is available at DOI: 10.1039/c3sm51650d.

14. ABSTRACT
Autonomic materials are those that automatically respond to a change in environmental conditions, such as temperature or chemical composition. While such materials hold incredible potential for a wide range of uses, their implementation is limited by the small number of fully-developed material systems. To broaden the number of available systems, we have developed a post-functionalization technique where a reactive Ru Catalyst ink is printed onto a non-responsive polymer substrate. Using a succinimide– amine coupling reaction, patterns are printed onto co-polymer or biomacromolecular films containing primary amine functionality, such as polyacrylamide (PAAm) or poly-N-isopropyl acrylamide (PNIPAAm) copolymerized with poly-N-(3-Aminopropyl)methacrylamide (PAPMAAm). When the films are placed in the Belousov–Zhabotinsky (BZ) solution medium, the reaction takes place only inside the printed nodes. In comparison to alternative BZ systems, where Ru-containing monomers are copolymerized with base monomers, reactive printing provides facile tuning of a range of hydrogel compositions, as well as enabling the formation of mechanically robust composite monoliths. The autonomic response of the printed nodes is similar for all matrices in the BZ solution concentrations examined, where the period of oscillation decreases in response to increasing sodium bromate or nitric acid concentration. A temperature increase reduces the period of oscillations and temperature gradients are shown to function as pace-makers, dictating the direction of the autonomic response (chemical waves).

15. SUBJECT TERMS
accoustically-based, thermal

16. SECURITY CLASSIFICATION OF:			17. LIMITATION OF ABSTRACT	18. NUMBER OF PAGES	19a. NAME OF RESPONSIBLE PERSON *(Monitor)*
a. REPORT	b. ABSTRACT	c. THIS PAGE	SAR	12	Richard A. Vaia
Unclassified	Unclassified	Unclassified			19b. TELEPHONE NUBER *(include area code)* (937) 255-9209

REPORT DOCUMENTATION PAGE Cont'd

6. AUTHOR(S)

R. A. Vaia - Materials and Manufacturing Directorate, Air Force Research Laboratory, Functional Materials Division
R. C. Kramb and P. R. Buskohl – UES, Inc.
C. Slone - Department of Material Science and Engineering, The Ohio State University
M. L. Smith - Department of Engineering, Hope College

7. PERFORMING ORGANIZATION NAME(S) AND ADDRESS(ES)

AFRL/RXA
Air Force Research Laboratory
Materials and Manufacturing Directorate
Wright-Patterson Air Force Base, OH 45433-7750

UES, Inc.
Dayton, OH 45432

Department of Material Science and Engineering
The Ohio State University
Columbus, OH 43210

Department of Engineering
Hope College
Holland, MI 49423

Soft Matter

PAPER

View Article Online
View Journal | View Issue

Autonomic composite hydrogels by reactive printing: materials and oscillatory response†

Cite this: *Soft Matter*, 2014, **10**, 1329

R. C. Kramb,[ab] P. R. Buskohl,[ab] C. Slone,[ac] M. L. Smith[ad] and R. A. Vaia*[a]

Autonomic materials are those that automatically respond to a change in environmental conditions, such as temperature or chemical composition. While such materials hold incredible potential for a wide range of uses, their implementation is limited by the small number of fully-developed material systems. To broaden the number of available systems, we have developed a post-functionalization technique where a reactive Ru catalyst ink is printed onto a non-responsive polymer substrate. Using a succinimide–amine coupling reaction, patterns are printed onto co-polymer or biomacromolecular films containing primary amine functionality, such as polyacrylamide (PAAm) or poly-*N*-isopropyl acrylamide (PNIPAAm) copolymerized with poly-*N*-(3-Aminopropyl)methacrylamide (PAPMAAm). When the films are placed in the Belousov–Zhabotinsky (BZ) solution medium, the reaction takes place only inside the printed nodes. In comparison to alternative BZ systems, where Ru-containing monomers are copolymerized with base monomers, reactive printing provides facile tuning of a range of hydrogel compositions, as well as enabling the formation of mechanically robust composite monoliths. The autonomic response of the printed nodes is similar for all matrices in the BZ solution concentrations examined, where the period of oscillation decreases in response to increasing sodium bromate or nitric acid concentration. A temperature increase reduces the period of oscillations and temperature gradients are shown to function as pace-makers, dictating the direction of the autonomic response (chemical waves).

Received 14th June 2013
Accepted 1st October 2013

DOI: 10.1039/c3sm51650d

www.rsc.org/softmatter

1 Introduction

Autonomic materials are those that automatically respond to a change in environmental conditions. These materials "sense" the environment as an input signal and respond accordingly without an external guide making decisions on their behalf. Living organisms represent the most complex examples of autonomic systems. However, simpler autonomous materials also exist, where one or more type of response is coupled with one or more environmental condition(s).[1] Depending on the properties of the autonomous material, potential for a wide range of devices has been discussed, such as energy storage, actuation, computation, self-repairing coatings, and encryption.[2,3] Yet, many issues must be understood before one can design and engineer a material with a desired autonomic response. For example, what are the relationships between transport, autonomic response and mechanical properties of the material that limit the size or shape change caused by the environment-response relationship? What is the relationship between shape, pattern and time scale associated with the response? How can multiple responses be constructively coupled within a single material? These challenges along with practical issues such as material durability and handleability necessitate the further development of new material systems with facile processing and composition control, as well as the continual development of theory and modeling tools.

The development of a sub-class of autonomic hydrogels that convert chemical energy into an optical or mechanical response has received substantial attention recently.[1,3–8] Such biocompatible hydrogels have the potential for use in biomedical applications including biomimetic valves (*e.g.* artificial heart), drug release, separation systems, and artificial skin. Other device applications include microfluidics (actuators) and micromachines (mass transport).[1] These polymer-based systems typically respond to variations in one or more environmental conditions, such as temperature, pH, light, concentration gradient, or electrical pulse; with a response including changes in size, shape or color.[1] The most studied autonomic hydrogels are based on poly(*N*-isopropylacrylamide) (PNIPAAm) and the Belousov–Zhabotinsky (BZ) reaction.[1] The oscillating BZ reaction occurs in a solution of sodium bromate (SB), malonic acid (MA), and nitric acid (NA), and is characterized by the periodic oxidation and reduction of a metallic catalyst (typically Ru between the (II) and (III) oxidation states).[9–12] When the metal

[a]*AFRL/RX Materials & Manufacturing Directorate, Air Force Research Laboratory, Wright-Patterson AFB, OH 45433, USA. E-mail: richard.vaia@us.af.mil*

[b]*UES, Inc., Dayton, OH 45432, USA*

[c]*Department of Material Science and Engineering, The Ohio State University, Columbus, OH 43210, USA*

[d]*Department of Engineering, Hope College, Holland, MI 49423, USA*

† Electronic supplementary information (ESI) available. See DOI: 10.1039/c3sm51650d

catalyst is incorporated into PNIPAAm-based gels, the periodic oscillation of its oxidation state alters the hydrophobicity of the hydrogel. The Ru(III) state is more hydrophilic than the Ru(II) state and therefore the PNIPAAm swells when the catalyst is oxidized.[1,10,13] A corresponding change in size or shape of the hydrogel occurs in phase with the BZ reaction.[1] For PAAm-based gels, an alternate mechanism has been proposed where interchain interactions cause the gel to swell for Ru(II), and deswell for Ru(III).[14] Overall, the extent of swelling in these autonomic hydrogels depends on factors including the total polymer concentration, the catalyst concentration, the crosslinking density, and the temperature of the reaction.[1]

Composite BZ hydrogels are the next step toward devices. These hydrogels contain both oscillatory (active) and non-oscillatory (non-active) regions in the same material.[2,15–17] Communication between the active nodes occurs *via* chemical and mechanical waves traveling through the inactive regions. Subsequent oscillatory synching of the active regions leads to emergent behavior and greatly increases the complexity and functionality of the autonomic response. Elucidating the design rules associated with building these composite hydrogels has been the focus of recent experiments and simulations.[1,15,18–20] The details of internode communication depends on the properties of the hydrogel and the geometry of node arrangement.[15] Photo illumination can also be used to modulate internode activity and overall composite behavior.[21–24] For example, inter-band transitions within Ru from absorption of 436 nm light inhibit BZ oscillations and enables continuous grey scale tuning of the reaction and the hydrogel response. By combining these concepts, wormlike motion and rudimentary swarming have been predicted.[21,22]

Unfortunately, the materials available to construct composite hydrogels with requisite mechanical robustness, simple fabrication, and precision of node geometry are limited.[1,11,20] The majority of BZ gel demonstrations in the literature are based on PNIPAAm as a monolithic cube, film, sphere, or cylinder of tens of microns to a few millimeters in size.[1] Recent approaches to overcome these limitations include using base polymers with more robust mechanical properties such as polyacrylamide (PAAm)[14,17] and gelatin,[2,15] and employing novel synthesis techniques and catalyst binding chemistries such as UV mask patterning,[14,17] and post-functionalization.[2,15] Of special note with regard to complex fabrication is the development of autonomic hydrogels compatible with additive processing (manufacturing) techniques. For example, the thermal gelation characteristics of gelatin enable printing of self-supporting structures by extruding hot gelatin (low viscosity) onto a cold substrate (high viscosity).[2,15] Glutaraldehyde crosslinking of co-printed, or printed and backfilled, structures of active (Ru-containing) and non-active gelatin result in monolithic systems. Printing thermogels can be challenging however due to their temperature sensitive viscosity. Current reports are limited to ~100 μm resolution, which may be inadequate for certain applications.[15]

To further expand the processing-material concepts for autonomic hydrogel fabrication, we demonstrate herein reactive printing of Ru-containing BZ–hydrogel composites. Using a succinimide–amine coupling reaction, responsive Ru patterns are embedded within co-polymer films containing primary amine functionality, such as PAAm or PNIPAAm copolymerized with *N*-(3-aminopropyl)methacrylamide (APMAAm). Reactive printing reduces the number of steps to create the active–inactive node patterns to two; one polymerization step to create a cross-linked monolithic film, and a second printing step to create the reactive patterns. The Ru catalyst is delivered in an ink solution of DMF, which can be applied with something as simple as a micro-dispenser or inkjet printer.

2 Experimental

2.1 Materials

N-Isopropyl acrylamide (NIPAAm), acrylamide (AAm), methylenebisacrylamide (MBA), ammonium persulfate (APS), tetramethylethylenediamine (TEMED), *N*,*N*-dimethylformamide (DMF), and bis(2,2′-bipyridine)-4′-methyl-4-carboxybipyridine-ruthenium *N*-succinimidyl ester-bis(hexafluorophosphate) (Ru(sbpy)) were purchased from Sigma-Aldrich and used as received. *N*-(3-Aminopropyl)methacrylamide hydrochloride (AMPAAm) was purchased from Polyscience, Inc. and used as received. For BZ reactants, sodium bromate (SB) and malonic acid (MA) were purchased from Sigma-Aldrich and used as received. Nitric acid (NA) was purchased from Sigma-Aldrich as 70% reagent and diluted to the concentration used in the reactions.

2.2 Reactive printing

Substrate polymers are fabricated into thin films ~400 μm thick by the following example procedure. 100 mg of AAm, 60 mg APMAAm, 3.2 mg MBA crosslinker, 5 mg APS, and 10 μL of TEMED were dissolved in 1 mL of deionized (DI) water. Other variations of this procedure include using NIPAAm in place of AAm, using a 90 : 10 mixture of NIPAAm–AAm, and adjusting the mass of MBA cross-linker, for example, to 1.6 mg. The solution was injected between two glass panels covered with hydrophobic BYTAC and separated by 4 BYTAC layers (~400 μm). This thickness provided adequate mechanical rigidity for subsequent handling and processing. The glass panels are clamped together and the film is allowed to polymerize for 4 hours at room temperature. After polymerizing, the film is allowed to dry for 20 minutes and cut with a razor blade into square sections approximately 2 cm × 2 cm. These square sections contain approximately 90% water by weight when fully hydrated. 1.5 mg of Ru(sbpy) catalyst is dissolved in 30 μL of DMF to make the reactive ink solution. For experiments to determine the period dependence on temperature and reactant concentration, one drop (approx. 5 μL) of reactive ink is applied by a microliter scale fluid dispenser equipped with a 26.5 gauge needle to the square section of the substrate to form a circular spot in the center with diameter ~1–2 mm. To demonstrate the ability to create complex shapes and patterns, we also printed spots of various sizes, lines, letters, and geometrical shapes such as squares, triangles and circles. The procedure used to print these shapes is the same as the 1–2 mm spots above, but the number of drops is either increased (for large spots) or the

drops overlapped each other to form a line (for lines and shapes). For line printing, a flow rate of 5 μL s^{-1} and a dispenser speed of 2 mm s^{-1} is used. After application of the ink, the substrates are placed in an oven at 35 °C and covered for 3 hours to allow the succinimide–amine coupling reaction to complete. By 3 hours, the films have dried to less than 5% water and the coupling reaction has completed. After this, they are rehydrated and washed with DI water to remove unreacted monomer and excess Ru(sbpy) until the wash no longer turns orange and remains clear. The washing process takes 5–10 cycles of immersing in ~10 mL of fresh water for 10 minutes followed by removal of the contaminated rinse.

2.3 Belousov–Zhabotinsky (BZ) driven oscillations

The printed sections are placed in a small Petri dish with 5 mL of BZ reactant solution and covered to prevent solvent evaporation. We note that failure to cover the reaction vessel results in solvent evaporation, and will lead to increasing reactant concentrations over time and an apparent long-time transitory behavior (time-dependent period of oscillations and shrinking of the hydrogel). In the BZ reaction, an organic compound (MA) is oxidized by an inorganic oxidant (SB), in the presence of a strong acid (NA) and a catalyst (Ru). BZ reactant concentrations range from 0.08–0.25 M for SB, 0.04–0.14 M for MA, and 0.5–1.1 M for NA with the base concentrations being 0.2 M (SB), 0.1 M (MA) and 1.0 M (NA). One reactant is varied at a time while the others are kept at the base concentration in order to determine the effect of each individual reactant on the period of chemical waves. Once in the BZ solution, the color of the spots changes from orange to transparent as the Ru oscillates between the (II) and (III) oxidation states, respectively. The BZ reaction is observed as swirls or lines of color that transverse the spots at regular intervals and are captured by images taken with a Dino-Lite microscope camera spaced 2 s apart. Total image acquisition and reaction time is 5 hours. The temperature of the reaction is controlled with a Peltier heating plate under the Petri dish connected to a variable voltage DC power source and monitored by a thermocouple adhered to the plate. The Dino-Lite camera images are separated into red, green and blue channel 8-bit images and the intensity of a single pixel of the blue channel is analyzed in Matlab to find the frequency of the color oscillations. The exact location of the pixel chosen on the printed spot had no effect on the results.

3 Results and discussion

3.1 Reactive printing

A diagram demonstrating the ink printing procedure and the succinimide–amine coupling reaction between Ru(sbpy) and APMAAm units is shown in Fig. 1. In brief, the succinimide–amine reaction forms an amide bond between the nitrogen atom in the amine group on the co-polymer and the acyl residue on the Ru complex. The reaction takes place in water and is most efficient at pH ~7–8 and temperatures ~40 °C.[15,25] A side hydrolysis reaction of the ester group competes with the amide bond formation in water which lowers the conjugation yield.

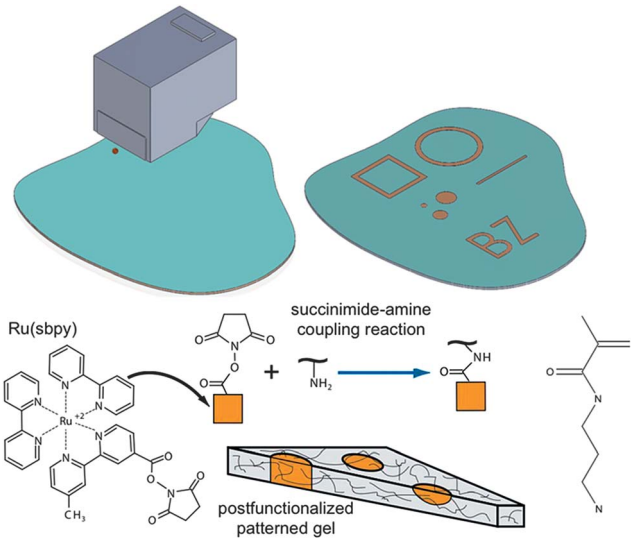

Fig. 1 (Above) Schematic diagram of the reactive printing procedure. Patterns can be programed by an ink jet printer, and complex patterns such as spots, lines, shape outlines, and letters have been printed. (Below) Diagram showing the succinimide–amine coupling reaction adapted from ref. 27. The succinimide–ester functional group on the Ru complex reacts with the amine groups of the APMAAm units along the co-polymer, which forms an amide bond that couples the Ru to the matrix. The structure of APMAAm is also shown.

Herein a microliter dispenser with a 26.5 gauge needle was used to meter 5 μL drops to produce pixelated patterns. Uniform lines were created by correlating the rate of fluid dispensing (5 μL s^{-1}) with lateral translation (2 mm s^{-1}). The process could be easily integrated into a programmable ink jet printer allowing a nearly limitless number of shapes and sizes of reactive patterns.[26] Examples of shapes and letters printed with this procedure are shown in Fig. 2, and a movie showing how the printed "letters" behave in the BZ reaction is found in the ESI, Movie S1.† Four key factors determine the response of these printed composite hydrogel patterns in the BZ solution. As

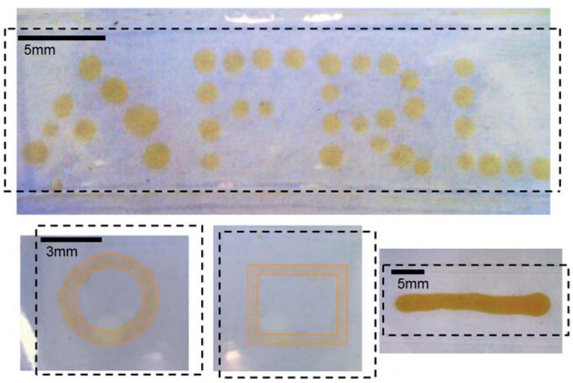

Fig. 2 Examples of shapes printed onto PAAm-*co*-APMAAm substrates using the procedures described in the text. Dashed black outlines have been drawn on the images to show the edge of the substrate material in solution and to clarify film borders due to reflections. Solid orange lines have been drawn on the circle and square printed shapes to help show where the ink was placed.

discussed in the following sections, these include the depth or penetration of the printed features, the concentrations of BZ reactants, the mechanical properties of the substrate material, and the temperature of the reaction.

3.2 Feature depth

The lateral size, and most importantly depth, of the printed active node depends on the extent to which the catalyst-containing ink diffuses into the substrate material. The profile will influence reaction kinetics since reactant diffusion rates are slower inside the polymer matrix than at the surface. It also determines whether the chemical waves are occurring at the film surface or in the bulk, and strongly influences the mechanical response of the active–inactive patterns, as the inactive volume below the active node will act as a constraining boundary to the autonomic swell–deswell behavior. In general, the profile of the printed node is directly related to the mutual solubility of the reactive Ru(sbpy), the ink, and the slightly swollen hydrogel substrate. If the polymer and Ru(sbpy) are both soluble in the solvent used for the ink, the printed feature will quickly spread, but also penetrate deeply into the hydrogel network. This solubility combination will maximize the total Ru(sbpy) incorporated into the hydrogel before hydrolysis deactivates the coupling reaction between pendent amine and Ru(sbpy), but will compromise the ability to print well-defined features. As an optimization trade, the inks formulated for Fig. 2 used DMF, a solvent in which PAAm and PNIPAAm has low solubility.[28] The edges of these printed features are crisp and well-defined. However, since the DMF solution does not readily diffuse into the polymer, the coupling reaction only takes place near the surface. The reactive ink penetrates only to a depth of 10–20 μm, as demonstrated in the cross section of a printed active node within PAAm-*co*-APMAAm shown in Fig. 3. Depending on the intended application, it is likely that the reactive ink can be formulated to be optimized for a given substrate and the required lateral and depth resolution of the active node by modifying co-solubility (*e.g.* DMF : water ratio of ink),[28] Ru(sbpy) concentration in the ink,[2,29] polymer concentration in the substrate (water content of film), and the ratio of APMAAm to base polymer in the hydrogel.

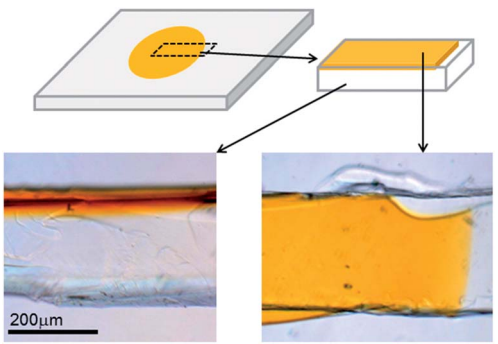

Fig. 3 Profile of reactively printed active node. An active node in PAAm-*co*-APMAAm substrate material was cut into a strip and optical microscope images were taken of the top and side faces. The cross sectional side face image shows the penetration depth of the ink of approximately 10–20 μm and the top face shows the well-defined border of the printed node.

3.3 Oscillation behavior of composite BZ hydrogel

The oscillation behavior of the printed composite hydrogel depends on the reactant concentration of the BZ solution, the mechanical characteristics of the composite, and temperature.[1] The dependence on reactant concentration and temperature provide potential means to control the period of oscillation across the nodal array by making uniform changes to these inputs. Using gradients, such as with temperature, provides control of the direction of the chemical waves.

Fig. 4 summarizes the dependence of the oscillatory behavior at 20 °C of single active nodes on the concentration of BZ chemical reactants. The reactant concentrations were varied individually while holding the other two reactants constant at the base concentration (see Experimental section). The relationship between the period and reactant concentration is given by the equation $P = A[SB]^b[MA]^c[NA]^d$ where P is the period, A is a reaction coefficient and b, c, and d are exponents independent of the other reactant concentrations. As shown by Smith and coworkers with gelatin[2] and Yoshida and coworkers with PNIPAAm,[11,30] the response empirically collapses to a single plot by using a sum of logs, $P = b\ \ln[SB] + c\ \ln[MA] + d\ \ln[NA]$. Overall, the period shortens with increasing reactant concentrations. However, the period has a much stronger dependence on SB and NA than MA. The series of images at the top of Fig. 4 show a

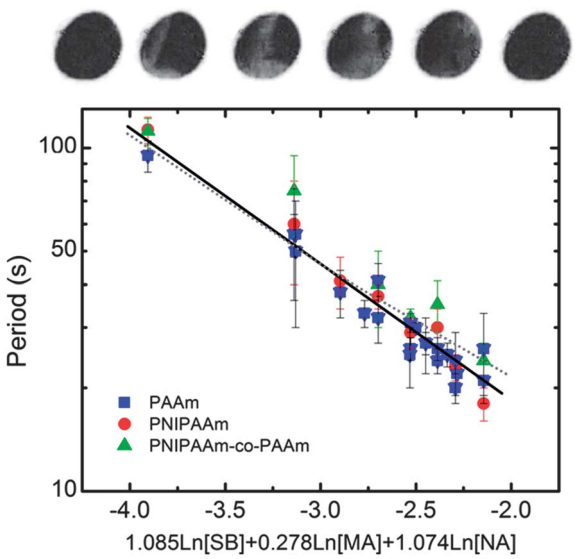

Fig. 4 Period of oscillations at 20 °C of printed active nodes (2–5 mm) in various hydrogels. Each hydrogel contains 38% by weight of APMAAm co-monomer. The concentrations of the BZ reactants are varied from 0.08–0.25 M for [SB], 0.04–0.14 M for [MA], and 0.5–1.1 M for [NA]. The solid line represents the nonlinear least squares fit to the period based on the reactant concentrations expressed as a sum of logs. The dashed line represents the behavior of the BZ reaction in the absence of hydrogel and with the same concentration of unbound Ru catalyst.[30] The series of images in the inset show an example of a chemical wave traveling across a printed node. Error bars indicate variation of the period within one experiment.

representative single wave response moving across an active node of PAAm-*co*-APMAAm. The color has been converted to greyscale to enhance the contrast between the (II) state, in black, and (III) state, in white. An example of the color oscillations over time of a printed spot are shown in the ESI, Fig. S1† and a movie showing an example of the behavior for a spot is shown in Movie S2.†

No significant difference in oscillatory behavior was found between reactively printed nodes in PAAm-*co*-APMAAm, PNIPAAm-*co*-APMAAm, and a 10 : 90 copolymer of PAAm and PNIPAAm. Each hydrogel contains 38% by weight of APMAAm. Repeated experiments indicate that sources of non-negligible experimental scatter include fluctuations in lab temperature, lab humidity, and reactant concentrations. These occur during film synthesis, node printing, and preparation and storage of the BZ solution. However, the largest source of noise, as indicated by the error bars in Fig. 4, is the drift of the period length from cycle to cycle within a single experiment. Considering these points, the results with different substrate materials is remarkably consistent. Additionally, compared to the reported period of oscillation of free Ru catalyst within a BZ solution at the same temperature (dashed line, Fig. 4), there is again little difference with the overall trend of the data.[11,30] This implies that although the catalyst is chemically bound to the matrix, the reaction kinetics are no different than those found in a solution with unbound catalyst. Similar results for the period of oscillations were determined for lateral node diameters from 1 mm to 5 mm as well as for shapes and lines, even though the shape of the wave differed with the size and shape of the node (*i.e.* one directional waves *versus* spiral waves).

Elucidating the impact of matrix composition on oscillatory response is not straightforward, as crosslink and hydrogel concentration has also been shown to play a role. For example, previous studies with gelatin[2] demonstrated a different exponential dependence of the period on the reactant concentrations. The exponents for SB, MA and NA in gelatin were found to be −0.512, 1.387, and −0.348 for a 400 μm cube, which compares to 1.085, 0.278, and 1.074 for this work. At the pH of the BZ solution (1–2), gelatin is a charged polyelectrolyte due to ionization of amino acids residuals such as glycine, glutamic acid and alanine. Also, physical gelation of the gelatin creates a molecularly inhomogeneous network. Both factors could result in different diffusion characteristics for the BZ reactants. Extrapolating these prior observations to similar BZ reactant concentrations examined herein would predict larger periods in the range of 60–300 s. Similarly, reports by Yoshida and coworkers, using monolithic PNIPAAm gels with similar crosslinking and polymer concentrations, would imply long periods of 100–500 s.[11,28] However, experiments by Nuzzo and coworkers with PAAm monoliths with much higher crosslinking (∼12% by mass) than discussed here, reported similar period lengths in the range of 10–60 s.[14]

As such, there are two potential explanations for the similarity in chemical wave period shown in Fig. 4. One is that for the printed composite hydrogels, the reaction takes place only in the near surface region due to the limited penetration of the active node. Because of this, possible reduction of diffusion rates of the BZ reactants by the surrounding inactive hydrogel is not a factor. The comparable oscillation rate with free solution bolsters this explanation. Thus the "matrix independent response" is a geometrical effect. Alternatively, the relatively low matrix concentration (10% polymer by volume when hydrated) and neutrality of PAAm does not substantially hinder the diffusion of the BZ reactants relative to the surrounding aqueous solution. Prior permeability studies of interpenetrating PAAm–PNIPAAm hydrogels show that rates of water uptake and diffusion of tracer Orange II azo dye depend non-monotonically on temperature, crosslinking, and total polymer content.[31] However, at temperatures below the LCST (32 °C), gel permeability of swollen films of comparable polymer and crosslinking concentration used herein only displayed a small effect on the relative PNIPAAm composition. This implied that the impact of the matrix composition was secondary to the absolute polymer concentration in these formulations. Further studies using print-based fabrication techniques are required to sort out the interplay between the relative size and shape of the active node on the oscillatory behavior of the composite.

The reactively printed composite hydrogels displayed oscillatory strains up to 0.5%. This was irrespective of the extent of PNIPAAm incorporation into the PAAm polymer backbone. This is in contrast to reports of monolithic gelatin,[2] PNIPAAm,[1,10,30] and PAAm[14] based autonomic hydrogels, with oscillatory swelling range from 2–20%. As noted above, the limited penetrability of the Ru ink that results in the crisp pattern formation also hinders the ability to uniformly distribute the Ru catalyst throughout a monolith of sufficient thickness and robustness to handle. Attempts to apply ink to all sides of a cube (400 μm^3) resulted in a core–shell structure and no measurable swelling. As discussed, the printing depth of the Ru catalyst is inversely related to the precision of the print geometry. This is also effectively a trade-off between print precision and swell performance of the BZ gel. For comparison purposes we normalize print depth, h, by gel thickness, H, to define fractional penetration depth h/H. The print depth and gel thickness in our system are $h = 10$–20 μm and $H = 400$ μm respectively, resulting in penetration depths of less than 0.05.

Fig. 5 summarizes finite element (FE) simulations (see SI methods) to provide a better understanding of the bulk swelling behavior of notional BZ gel cubes with variable penetration depths of active isotropic material. As shown in Fig. 5A, we see that for a 0.05 penetration depth the swell ratio of the entire gel is low, even if the active material swells 10%. For an elastically incompressible material, bulk swelling performance is essentially a volume-weighted average of the active and non-active components. As the penetration depth of the active node decreases, the influence of the non-active underlying region is more pronounced. Bulk swelling could be increased by using a less stiff non-active gel. This however, will affect the overall mechanical robustness of the composite structure, potentially weakening it beyond practical transport and positioning requirements.

Fig. 5 also indicates that the swelling of the composite hydrogel is heterogeneous due to the constraint of the non-active material. This heterogeneity is distinctly seen in the drop

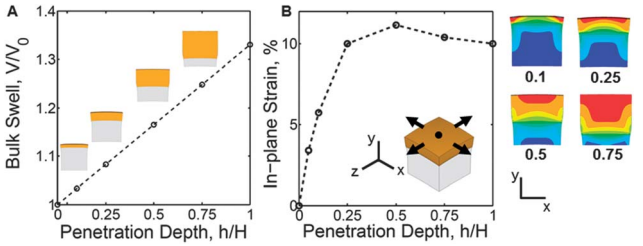

Fig. 5 Mechanical constraints on autonomic swell–deswell behavior of reactively printed node. (A). Bulk swell behavior transitions from constrained to free swelling as the active node penetrates the gel thickness, H. Insets show swollen configuration of varying penetration geometries. (B) Plot of in-plane strain ε_{xx} near the surface of the active material *versus* penetration depth. In-plane swelling (ε_{xx}, ε_{zz}) near the surface of the active material is constrained at low penetration depths. The black dot indicates where the strain values were taken. Figures to the right are contour plots of ε_{xx} for different h/H ratios showing strain distribution (uniform color gradient between red: 10% and blue: ≤0%).

of in-plane strains (ε_{xx}, ε_{zz}) in the center of the cube near the active material surface (Fig. 5B). The proximity of this top surface to the active–non-active interface at low penetration depths limits the in-plane strain of the active material. The strain normal to the surface (ε_{yy}) compensates for this constraint by swelling beyond the prescribed 10%, resulting in a mushroom geometry. As seen in the contour plot of Fig. 5B, the uniformity of the in-plane strain field in the active material increases as the penetration depth increases and the active–non-active interface moves farther away from the surface. Thus at short penetration depths, oscillation of surface "bumps" in the center of the active nodes is more likely than overall macroscopic strain of the composite hydrogel.

Recent studies indicate that mechanical forces can resuscitate chemical oscillations in BZ systems[20] and swelling may be able to coordinate the chemical oscillations of neighboring Ru nodes.[32] Mechanical triggering of neighboring nodes will likely require a minimal in-plane strain magnitude, which could be masked at low penetration depths by the non-active material. Compensatory swelling normal to the surface (ε_{yy}), will be ineffective at stimulating synch as its action is orthogonal to the plane of active nodes. Thus for optimal mechanical syncing of planar arrays, the active nodes should span the film thickness. Chemical synching of active nodes, which depends on reactant diffusivity, will be influenced more by relative placement of nodes than penetration depth. These trade-offs highlight the importance of clearly identifying the design objectives of a composite BZ device before selection of a fabrication technique and material.

Finally, control of the oscillation behavior of the reactively printed nodes, including both period and wave direction, is demonstrated in Fig. 6 and 7 through the use of a temperature jump or gradient. As an example, Fig. 6 summarizes the reversible oscillatory control of an active node in PAAm-*co*-APMAAm using a simple Peltier heating plate under the reaction dish ([SB] = 0.2 M, [MA] = 0.1 M, and [NA] = 1.0 M). Changes in the frequency of oscillations were observed within a few minutes of changing the temperature and were reversible.

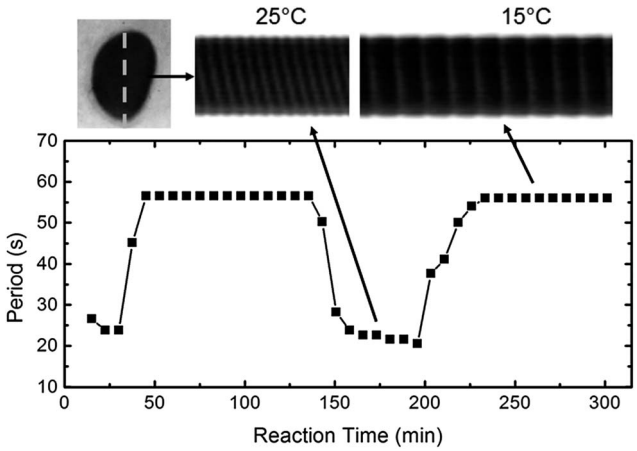

Fig. 6 Oscillatory control of active node in PAAm-*co*-APMAAm *via* temperature jump. The period of chemical waves reversibly changes with temperatures. Approximately 25 s periods are seen at 25 °C. At 15 °C the period lengthens to ~55 s, then returns to 20–25 s once a 25 °C temperature is restored. Finally, the period returns again to ~55 s periods at 15 °C. Inset shows the active node denoting the region (black line) in which the temporal behavior is displayed above the data. Node diameter is 2 mm and dark regions indicate (II) state while light regions indicate (III).

Specifically, 30 minutes after beginning the reaction, the temperature of the plate was changed from 25 °C to 15 °C. Then at 140 minutes from 15 °C to 25 °C, and finally at 200 minutes back to 15 °C. Within approximately 15 minutes of the temperature changes, the reaction reaches a new steady state with an oscillation period of 55 seconds (15 °C) or 25 seconds (25 °C). For these reactant concentrations and for temperatures between 15 °C and 35 °C, the period of oscillations was found to empirically follow an exponential dependence of the form

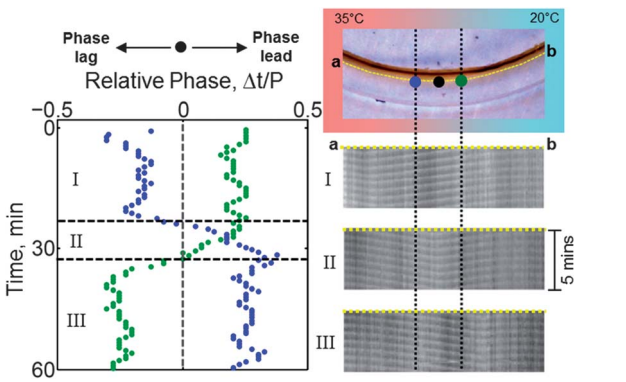

Fig. 7 Directional control of chemical wave in PAAm-*co*-APMAAm gel with temperature gradient. Plot of the relative phase lead and phase lag of Ru oxidation between the black center node and the outer green and blue nodes, which shows the transition from the initially longer right-to-left 20 °C waves to the shorter, edge-initiated, left-to-right 35 °C waves. The left side temperature was increased to 35 °C at nominal time equals zero. Phase is normalized to period length, P ($P \sim 35$ s at 20 °C). Schematic contains gel geometry and orientation of thermal gradient. Grayscale images show signal intensity along the yellow dashed line from (a) and (b), plotted in 5 minute sections.

$P = 5.7 \exp(30(1/T))$, where P = period in seconds, and T = temperature in °C. Recall PAAm does not exhibit a LCST such as seen in PNIPAAm.[33] Thus the temperature dependence is expected to follow BZ reaction behavior, which is typically Arrhenius-like.[1] Note that empirically similar temperature behavior has been seen for actuators made from PNIPAAm; however quick-responding reversibility was not demonstrated, which is most likely due to the hysteresis in swell–deswell behavior of the gel.[34]

The temperature dependence on the period can also be used to control the direction of the waves, as summarized in Fig. 7. A sample with a straight line was placed in the BZ solution with the Peltier plate set to a uniform 20 °C. At this uniform temperature there is no preference for the direction of the waves at steady state. In Fig. 7, the waves moved from right to left across the printed line. After reaching steady state, the left half of the film was placed onto a 35 °C plate, while the right half remained on the 20 °C plate. After an initial equilibration time, waves began initiating at the far left edge of the sample and moving from left to right at a shorter period, consistent with the temperature jump behavior in Fig. 6. Eventually the short left-to-right waves took over the longer right-to-left waves along the entire sample. The complete movie of this behavior is included in the ESI (Movie S3†). This transition in wave direction was quantified using the relative phases between the oxidation peaks measured at three uniformly spaced locations, denoted as the colored dots in the upper right of Fig. 7. Initially, the wave originates from the right side of the sample (green dot). Then from approximately 25 minutes to 32 minutes, BZ waves approach from both sides of the black node. Eventually the left (blue) side waves overcome the right (green) side and lead the wave direction. In other words, the high temperature (short period) side of the sample became a pacemaker for the rest of the sample. This is consistent with previous work that showed when nodes with two different frequencies are close enough to communicate (and in this case have no separation between the 35 °C side and the 20 °C side), the one with the shorter frequency acts as the pacemaker.[15,32] Further explanation of wave direction analysis is given in the ESI, including the Fig. S2.† Extending this into a 2D or 3D system could provide a unique means to convert multi-dimensional thermal information into an optical signal, with potential application as a thermocouple or anti-tampering sensor.

4 Conclusion

In this study, reactive printing is demonstrated as a facile means to create autonomic composite hydrogels. Using succinimide–amine coupling reaction and ink formation, fine detailed patterns of Ru(sbpy)-containing active regions are formed on substrates containing primary amines, such as PAAm and PNIPAAm hydrogels copolymerized with PAPMAAm. Importantly, we find that the period of the printed active node is not affected by the choice of substrate polymer and is not measurably different than that of the Ru catalyst in solution. This demonstrates that for these composite systems and polymer concentrations the chemical details of the hydrogel play a secondary role in the behavior. Thus autonomic response depends on extrinsic factors including the reactant concentrations, the structure of the active–inactive node, and temperature. For example, the node depth is limited to a small fraction of the overall hydrogel thickness due to a combination of factors including overall substrate thickness required for handling and a trade-off between ink penetration and precision feature printing. This constrains the swell–deswell behavior of the printed nodes, and thus mechanical swelling behavior was not observed in our composite hydrogels. Our findings suggest that to achieve swelling sufficient for two active nodes to communicate through strain distortions of an intervening inactive matrix, the minimum penetration depth is likely to be ~40% of the total thickness of the sample. Optimally, one would create a cylindrical pillar that extends the entire thickness of the sample. The reactive printing techniques described here though would not be suitable for such a design.

We demonstrate that temperature exponentially impacts the oscillation period within an active node. Temperature gradients direct wave propagation through stripes or arrays of active nodes. The shorter waves that originate at a higher temperature eventually dominate over those from lower temperature in a manner analogous to the pacemaker effect seen in high frequency nodes in close proximity.[15] This implies that inhomogeneities in temperature can be combined with mechanical swelling in a way similar to that discussed with photo illumination[21,22] to create directed motion and transport along BZ reactive strips.

The reactive Ru ink described here can be used to build complex patterns of active–inactive composite BZ hydrogels. This precise control of spatial patterning enables future studies into the interaction of Ru placement with other known triggers of the BZ system, such as light, temperature, and mechanical strain.[21,35,36] The primary limiting factor of this study was the trade-off between ink penetration and pattern precision. Future alternative Ru reactant and polymer chemistries may offer improved binding efficiency and solubility, which would help mitigate the penetration limitation. The merging of autonomic hydrogel composites with the rapid maturation of additive manufacturing tools, including inkjet printers, has vast potential due to the ease of programing and creating arbitrary 2D and 3D structures. In the future, by combining reactive printing with different solvents and substrates that enhance mechanical swelling, a new class of fast fabricated, autonomously shape changing devices can be envisioned.

Acknowledgements

The authors thank Christopher Bailey and Hilmar Koerner for experimental assistance with temperature control. Work at the Air Force Research Laboratory Materials and Manufacturing Directorate was supported through the Air Force Office of Scientific Research.

References

1 R. Yoshida, *Adv. Mater.*, 2010, **22**, 3463–3482.

2 M. L. Smith, K. Heitfield, C. Slone and R. A. Vaia, *Chem. Mater.*, 2012, **24**, 3074–3080.
3 K. S. Toohey, S. R. White, J. A. Lewis, J. S. Moore and N. R. Sottos, *Nat. Mater.*, 2007, **6**, 581–585.
4 T. Tanaka, in *Polyelectrolyte Gels*, American Chemical Society, Washington, DC, 1992.
5 E. S. Gil and S. M. Hudson, *Prog. Polym. Sci.*, 2004, **29**, 1173–1222.
6 S.-k. Ahn, R. M. Kasi, S.-C. Kim, N. Sharma and Y. Zhou, *Soft Matter*, 2008, **4**, 1151–1157.
7 P. Calvert, *MRS Bull.*, 2008, **33**, 207–212.
8 S. Ramakrishnan, V. Gopalakrishnan and C. F. Zukoski, *Langmuir*, 2005, **21**, 9917–9925.
9 A. N. Zaikin and A. M. Zhabotinsky, *Nature*, 1970, **225**, 535–537.
10 R. Yoshida, T. Takahashi, T. Yamaguchi and H. Ichijo, *J. Am. Chem. Soc.*, 1996, **118**, 5134–5135.
11 R. Yoshida, M. Tanaka, S. Onodera, T. Yamaguchi and E. Kokufuta, *J. Phys. Chem. A*, 2000, **104**, 7549–7555.
12 S. Nakamaru, S. Maeda, Y. Hara and S. Hashimoto, *J. Phys. Chem. B*, 2009, **113**, 4609–4613.
13 R. Yoshida, T. Sakai, S. Ito and T. Yamaguchi, *J. Am. Chem. Soc.*, 2002, **124**, 8095–8098.
14 P. Yuan, O. Kuksenok, D. E. Gross, A. C. Balazs, J. S. Moore and R. G. Nuzzo, *Soft Matter*, 2013, **9**, 1231–1243.
15 M. L. Smith, C. Slone, K. Heitfield and R. A. Vaia, *Adv. Funct. Mater.*, 2013, **23**, 2835–2842.
16 V. V. Yashin and A. C. Balazs, *Phys. Rev. E: Stat., Nonlinear, Soft Matter Phys.*, 2008, **77**, 046210.
17 V. V. Yashin, S. Seiichi, R. Yoshida and A. C. Balazs, *J. Mater. Chem.*, 2012, **22**, 13625.
18 O. Kuksenok, V. V. Yashin, P. Dayal and A. C. Balazs, *J. Polym. Sci., Part B: Polym. Phys.*, 2010, **48**, 2533–2541.
19 P. Dayal, O. Kuksenok, A. Bhattacharya and A. C. Balazs, *J. Mater. Chem.*, 2012, **22**, 241–250.
20 I. C. Chen, O. Kuksenok, V. V. Yashin, A. C. Balazs and K. J. Van Vliet, *Adv. Funct. Mater.*, 2012, **22**, 2535–2541.
21 P. Dayal, O. Kuksenok and A. C. Balazs, *Langmuir*, 2009, **25**, 4298–4301.
22 S. Shinohara, T. Seki, T. Sakai, R. Yoshida and Y. Takeoka, *Angew. Chem., Int. Ed.*, 2008, **47**, 9039–9043.
23 S. Kadar, T. Amemiya and K. Showalter, *J. Phys. Chem. A*, 1997, **101**, 8200–8206.
24 M. Jinguji, M. Ishihara and S. Nakamaru, *J. Phys. Chem.*, 1992, **96**, 4279–4281.
25 G. T. Hermanson, *Bioconjugate Techniques*, Elsevier, Amsterdam, 2008.
26 P. Krober, J. T. Delaney, J. Perelaer and U. S. Schubert, *J. Mater. Chem.*, 2009, **19**, 5234–5238.
27 M. L. Smith, K. Heitfield, M. Tchoul and R. A. Vaia, Chemical wave characterization of self-oscillating gelatin and polyacrylamide gels, *Proc. SPIE 7975, Bioinspiration, Biomimetics, and Bioreplication*, 2011, 79750A.
28 S. Wu and R. A. Shanks, *J. Appl. Polym. Sci.*, 2004, **93**, 1493–1499.
29 T. Masuda, M. Hidaka, Y. Murase, A. M. Akimoto, K. Nagase, T. Okano and R. Yoshida, *Angew. Chem., Int. Ed.*, 2013, **52**, 7468–7471.
30 R. Yoshida, O. Satoko, T. Yamaguchi and E. Kokofuta, *J. Phys. Chem. A*, 1999, **103**, 8573–8578.
31 M. R. Guilherme, R. da Silva, A. F. Rubira, G. Geuskens and E. C. Muniz, *React. Funct. Polym.*, 2004, **61**, 233–243.
32 V. V. Yashin and A. C. Balazs, *Phys. Rev. E: Stat., Nonlinear, Soft Matter Phys.*, 2008, **77**, 046210.
33 L. Wang, J. Wang, Y. Huang, M. Liu, M. Kuang, Y. Li, L. Jiang and Y. Song, *J. Mater. Chem.*, 2012, **22**, 21405–21411.
34 S. Maeda, Y. Hara, R. Yoshida and S. Hashimoto, *Macromol. Rapid Commun.*, 2008, **29**, 401–405.
35 V. V. Yashin, K. J. Van Vliet and A. C. Balazs, *Phys. Rev. E: Stat., Nonlinear, Soft Matter Phys.*, 2009, **79**, 046214.
36 I. C. Chen, O. Kuksenok, V. V. Yashin, A. C. Balazs and K. J. Van Vliet, *Adv. Funct. Mater.*, 2012, **22**, 2535–2541.